Hindawi
International Journal of Polymer Science
Volume 2019, Article ID 2751384, 9 pages
https://doi.org/10.1155/2019/2751384

Research Article

Alphastatin-Loaded Chitosan Nanoparticle Preparation and Its Antiangiogenic Effect on Lung Carcinoma

Li Zhang and Yaoren Hu

Second Hospital of Ningbo, Ningbo, China

Correspondence should be addressed to Yaoren Hu; hu510@126.com

Received 15 September 2018; Revised 15 December 2018; Accepted 24 December 2018; Published 7 April 2019

Guest Editor: Mingqiang Li

Alphastatin is a 24-amino acid peptide and can suppress tumor angiogenesis by inhibiting both the migration and tubule formation of vascular endothelial cells. However, the anticancer effect of Alphastatin is limited due to the short half-life and degradation in the body. In this study, Alphastatin-loaded chitosan nanoparticles (AsCs NPs) were prepared with an initial concentration of 2 mg/ml for chitosan and 1 mg/ml for Alphastatin. AsCs NPs presented the encapsulation efficiency of 32.4%, the mean particle size of 387.4 nm, the polydispersity index of 0.223, and the zeta potential of +28.1 mV. AsCs NPs have a sustained release for 6 days and were stable in serum for at least 24 hours. And the NPs could preserve the integrity of encapsulated Alphastatin and released Alphastatin for 24 hours. In a subcutaneous LA975 lung carcinoma xenograft T739 mouse model, AsCs NPs significantly inhibited the tumor growth, tumor volume, and microvessel density (MVD), and the antitumor effect was even stronger than that of Alphastatin. In addition, the VEGF-induced tube formation of HUVEC could be inhibited by AsCs NPs *in vitro* and the serum containing AsCs NPs, and the protein level of SphK1 in HUVEC was also decreased by AsCs NPs, suggesting an inhibitory effect of AsCs NPs on the SphK1-S1P signaling pathway. Furthermore, hemolysis assay showed a safety on blood compatibility of AsCs NPs. Our study indicated that AsCs NPs inhibited the SphK1-S1P signaling pathway and enhanced the antiangiogenic effect of Alphastatin both *in vitro* and *in vivo*.

1. Introduction

Lung cancer is a serious and life-threatening malignant tumor. Though great progress has been made in detection and treatment, the 5-year survival rate of lung cancer remains less than 15%. The invasion and metastasis of tumor are the underlying causes of treatment failure and mortality, and angiogenesis is the prerequisite and foundation for invasion and metastasis of tumor cells [1]. Thus, inhibition of tumor angiogenesis has emerged as an important strategy for antitumor therapy. Alphastatin is a designed and synthetic peptide containing 24 amino acids [2], whose structure is according to the fibrinogen E fragment (FgnE), a potent antiangiogenic factor [3]. It has been reported that Alphastatin acts on activated vascular endothelial cells in the tumor to inhibit tumor angiogenesis [4]. However, as a peptide, due to easy degradation by widely distributed proteolytic enzymes, Alphastatin has a short half-life; therefore, its antitumor angiogenesis could not be fully exerted [5].

Chitosan is a natural cationic polysaccharide and has been widely used as a biomaterial due to its chemical stability, safety, nontoxicity, biocompatibility, and biodegradability. Chitosan is often used as a carrier material to prepare drug-loaded nanoparticles [6]. Previous studies have shown that chitosan can entrap protein and peptide drugs and protect them from hydrolysis by proteolytic enzymes, so that the drug retention time in the body can be prolonged [7]. In addition, the preparation method of drug-loaded chitosan nanoparticles is relatively simple with moderate conditions. And the process has little effect on the bioactivity of proteins or peptides because organic solvent is not involved. Moreover, it has been reported that chitosan and its derivatives have inhibitory effects on cervical cancer, gastric cancer, and other tumor cells.

In view of the excellent carrier properties of chitosan, we speculated that Alphastatin-loaded chitosan nanoparticles (AsCs NPs) may enhance the antitumor effect of Alphastatin. In this study, AsCs NP was prepared and its efficacy against tumor angiogenesis was investigated both *in vivo* and *in vitro*.

2. Materials and Methods

2.1. Materials. Unless stated otherwise, all chemical reagents were purchased from Sigma-Aldrich. Chitosan has a 95% deacetylation degree and 100 kDa of average molecular weight. Alphastatin was purchased from GL Biochem (Shanghai) Ltd., and the amino acid sequence is ADSGEGDFLAEGGG VRGPRVVERH. 2 mice bearing LA975 lung tumor and 44 T739 mice were purchased from the Center for Laboratory Animals, Ningbo University. The T739 mice were 5 weeks old. The mice were all bred in a specific pathogen-free (SPF) room. Human umbilical vein endothelial cells (HUVECs) were obtained from Fuyang Biotech (Shanghai, China). Matrigel was purchased from Corning Inc. (Shanghai, China). The EGM2 medium was purchased from Lonza.

2.2. Preparation of AsCs NPs and Measurement of Encapsulation Efficiency (EE%). Different final concentrations of chitosan at 1.0 or 2.0 mg/ml were dissolved in acetic acid solution (0.1 M, pH = 5.0). 4 ml of chitosan/acetic acid solution was taken, and then a high concentration of Alphastatin was slowly added. The different mass ratios of chitosan to Alphastatin at 1 : 4, 1 : 2, 1 : 1.5, 1;1, 2 : 1, 4 : 1, and 8 : 1 were produced, corresponding to final concentrations of Alphastatin at 8 mg/ml, 4 mg/ml, 3 mg/ml, 2 mg/ml, 1 mg/ml, 0.5 mg/ml, and 0.25 mg/ml. After mixing well and incubating overnight at room temperature, 2.0 mg/ml sodium tripolyphosphate (TPP) was slowly added into the solution under magnetic stirring to a 4 : 1 mass ratio of chitosan to TPP, and the mixture was stirred continuously for 30 min. Then, the mixture was centrifuged at 4°C, 13,000 g for 30 min, and the sediment was collected. The sediment was resuspended in deionized water and lyophilized by freeze-drying. The powder was named AsCs NPs. Similarly, the blank chitosan nanoparticles (Cs NPs) were prepared following the above process without adding Alphastatin.

For EE% measurement, after adding TPP and stirring for 30 min, the mixture was centrifuged at 4°C, 13,000 rpm for 30 min, then the supernatant was collected and the protein concentration of free Alphastatin was measured using the colorimetric bicinchoninic acid (BCA) method according to the protocol provided with the BCA assay kit (Thermo Fisher). EE% was calculated according to the following formula, and the supernatant from the blank chitosan mixture without Alphastatin was set as the blank control.

$$\text{EE\%} = 100\% \times (\text{total amount of alphastatin used} - \text{amount of free alphastatin}) \div \text{total amount of alphastatin used}. \quad (1)$$

2.3. Nanoparticle Characterization. The nanoparticle size, polydispersity index (PDI), and surface charges were determined in water by using the DelsaNano C particle size and zeta potential analyzer (Beckman Coulter, CA, USA).

2.4. Morphology. Transmission electron microscopy (Philips CM12, Eindhoven, Netherlands) was used to examine the morphology of AsCs NPs developed in this study. Before microscopy observation, the NPs were stained with 2 wt% of phosphotungstic acid and placed on a copper grid coated with Formvar/carbon films.

2.5. In Vitro Drug Release. AsCs NPs was prepared with 2.0 mg/ml chitosan and 1 mg/ml Alphastatin in a mixture (a 2 : 1 mass ratio of chitosan to Alphastatin), and the mixture was centrifuged at 13,000 rpm for 30 min and lyophilized to obtain the powder. 2 mg AsCs NPs was precisely weighed and mixed in 10 ml PBS (pH = 7.4). The mixture was placed in a constant temperature shaker at 37°C and 200 rpm/min. At various intervals of 1 hour, 2 hours, 4 hours, 8 hours, 12 hours, 24 hours, 48 hours, 96 hours, and 144 hours, the mixture was centrifuged for 30 min (13,000 rpm), then 2 ml supernatants were collected and 2 ml fresh PBS was added to the mixture. Then, the concentrations of free Alphastatin were determined using the BCA method.

2.6. Stability Study of the AsCs NPs in Serum. 1 mg AsCs NPs (a 2 : 1 mass ratio of chitosan to Alphastatin in preparation) were precisely weighed and mixed in 5 ml DMEM medium containing 10% fetal bovine serum (FBS). Then, the mixture was placed in an incubator at 25°C or 37°C. At various intervals of 0 hours, 4 hours, 8 hours, 16 hours, and 24 hours, mixtures in different tubes were centrifuged and lyophilized and the nanoparticle size was measured.

2.7. Integrity Study of Alphastatin. 2 mg AsCs NPs were weighed, mixed in 2 ml PBS (pH = 7.4), placed at 37°C, and shaken at 200 rpm/min. After 24 hours, the mixture was centrifuged for 30 min at 13,000 rpm. The supernatant and the sediment were collected. Then, the synthetic Alphastatin, supernatant, and sediment were analyzed by Tricine-sodium dodecyl sulfate-polyacrylamide gel electrophoresis (Tricine-SDS-PAGE) using a 16.5% gel [8]. The molecular mass of samples was investigated compared with the ultra low range molecular weight marker of MW 1060–26,600 (M3546, Sigma). Peptides were stained with 0.2% Coomassie Brilliant Blue G-250 (Sigma).

2.8. Tumor Model and Treatments. The study was approved by the Ningbo University Institutional Animal Care and Use Committee (Ningbo, China). 2 mice have been

subcutaneously implanted with LA975 cells, and the tumors have grown for 2 weeks. The tumor-bearing mice were sacrificed, and the tumors were stripped and weighed. After washing twice with PBS, sterile saline was added at a mass-to-volume ratio of 1 g tumor to 4 ml saline. Then, the tumor was grounded using the syringe, and the mixture was filtered by a 200-mesh sieve to make a suspension of single cells. The cell density was diluted to 1×10^7 cells per ml. Then, each T739 mouse was subcutaneously implanted with 0.2×10^7 cells in 0.2 ml in the lower dorsal region. After 10 days of injection, 24 T739 mice were randomly divided into 4 groups with half female and half male: saline group (0.2 ml saline/day), Alphastatin group (0.25 mg/kg/day), AsCs NP group (AsCs NPs containing 0.25 mg Alphastatin for one kg weight, once a day), and Cs NP group (Cs NPs containing the same amount of chitosan as in the AsCs NP group, once a day). The reagents were all intravenously injected once daily for 14 consecutive days.

2.9. Quantification of Tumor Microvessel Density (MVD). Tumors were fixed by formalin and cut into 5 μm frozen sections. Immunohistochemistry was performed using the monoclonal antibody against Factor VIII (DAKO) specific for endothelial cells of microvessels [9] and visualized by the streptavidin–peroxidase conjugated method. MVD was assessed according to the literature previously reported [10]. Briefly, the most vascularized intratumoral area was scanned under low magnification. The number of factor VIII-positive vessels was counted in 10 randomly hot spot areas under 400x magnification. Then, the mean value was calculated from 3 images under low magnification.

2.10. Preparation of Serum Containing AsCs NPs. 20 T739 mice were randomly divided into 4 groups and administrated by intravenous injection once daily for 14 consecutive days with saline (0.2 ml saline/day), Alphastatin (0.25 mg/kg/day), AsCs NPs (AsCs NPs containing 0.25 mg Alphastatin for one kg weight), or Cs NPs (Cs NPs containing the same amount of chitosan as it in AsCs NPs group). On the last day, after 2 hours of injection, blood samples were collected by removing the eyeball from mice, immediately centrifuged at 3,000 rpm for 15 min. Then, the serums were stored at 4°C immediately.

2.11. HUVEC Tube Formation Assay. Matrigel assay was performed in a 96-well plate as described previously [11]. Briefly, 80 μl Matrigel was added into each well of the 96-well plate and incubated at 37°C for 45 min for hardening. HUVEC was trypsinized and washed by PBS. The cell density was diluted to 3×10^5 per ml using EGM2 medium. 100 μl cells were added into the Matrigel-precoated plate. Saline, 100 nM Alphastatin, AsCs NPs containing 100 nM Alphastatin, and Cs NPs containing the same amount of chitosan were added to individual wells. For the serum sample test, different serums were diluted to 20% final concentration. Then, the plate was incubated at 37°C for 24 hours. Images of the HUVEC tube-like structure were then captured under a digital microscope, and the mean tube length was calculated.

2.12. Western Blot Assay. HUVEC was trypsinized, washed by PBS, and diluted to 3×10^5 per ml using EGM2 medium. 100 μl cells were added into each well of the 96-well plate. After overnight incubation, the medium was replaced with EGM2 containing saline, 100 nM Alphastatin, AsCs NPs containing 100 nM Alphastatin, or Cs NPs containing the same amount of chitosan. Then, the plate was incubated at 37°C for 24 hours. The protein was extracted using ice-clod RIPA lysis buffer. 20 μg proteins were kept 5 min in boiling water, separated by gel electrophoresis, and then transferred to polyvinylidene fluoride (PVDF) membranes. After blocking, PVDF membranes were incubated with primary antibody, anti-SphK1 (1 : 500, Santa Cruz Biotechnology), and anti-β-actin (1 : 1000) at 4°C overnight. Furthermore, the membranes were washed and incubated with HRP-conjugated secondary antibodies (1 : 10,000) at room temperature for 2 hours. Then the bands were visualized using ECL chemiluminescence reagents (Pierce, USA) and quantified using Image-Pro Analysis software.

2.13. Hemolysis Assay. The heparinized blood was drawn from healthy mice and centrifuged at 1000 rpm for 5 min to collect the packed red blood cells (RBC). The RBC was washed three times with isotonic saline buffer with pH 7.4 before diluting to prepare 2% erythrocyte dispersion. Hemolysis assay was studied by adding 500 μl RBC to the equal volume of CS and AsCs NPs in isotonic saline buffer to get a final concentration of 0.1 mg/ml, 0.05 mg/ml, and 0.025 mg/ml of polymer. The distilled water (100% hemolysis) and isotonic saline buffer (0% hemolysis) were employed as the positive and negative control, respectively. After incubation for 2 hours at 37°C, the mixtures were centrifuged at 1,000 rpm for 5 min. The obtained supernatant determined the absorbance at 545 nm. The hemolysis ratio (HR%) was calculated according to $\text{HR\%} = 100\% \times (\text{OD}_{\text{Sample}} - \text{OD}_{\text{negative}}) \div (\text{OD}_{\text{positive}} - \text{OD}_{\text{negative}})$.

2.14. Statistical Analysis. Quantitative data were expressed as mean ± SD. All analyses were performed by using Prism software (GraphPad 5.0). The statistical differences were determined by Student's t-test or one-way ANOVA, with $P < 0.05$ considered statistically significant.

3. Results and Discussion

3.1. The Effect of the CS/Alphastatin Ratio on EE%. In order to prepare chitosan nanoparticle-loaded adequate amounts of Alphastatin, we used EE% as a detection index and focused on investigation of the effect of the mass ratio of chitosan and Alphastatin to EE%. As shown in Figure 1, we found a significant EE% increase along with the increase in the mass ratio of chitosan to Alphastatin. When the chitosan concentration was 1.0 mg/ml and the CS/Alphastatin ratio was 8 : 1, EE% of chitosan to Alphastatin could increase to 40.2%. When the chitosan concentration was 2.0 mg/ml and the CS/Alphastatin ratio was 8 : 1, EE% could increase to 51.2%. Furthermore, when the CS/Alphastatin ratio was greater than 1 : 1.5, EE% from the 2.0 mg/ml chitosan concentration was always higher than EE% from the 1.0 mg/ml chitosan concentration, although both EE% decreased dramatically when the ratio

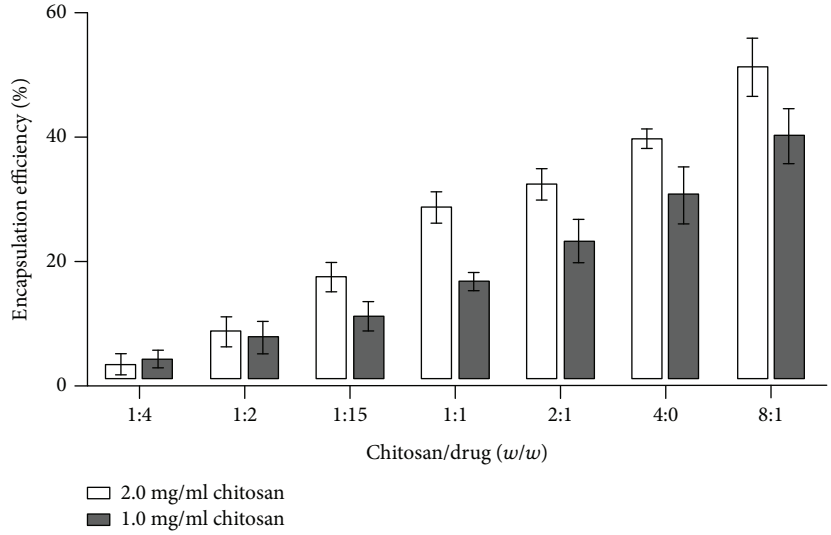

Figure 1: Effect of the mass ratio of chitosan to Alphastatin on Alphastatin encapsulation efficiency (%).

Table 1: Effect of the mass ratio of chitosan to Alphastatin on nanoparticle size and zeta potential. Chitosan concentration is 2 mg/ml.

	Mass ratio of chitosan to Alphastatin						
	1 : 4	1 : 2	1 : 1.5	1 : 1	2 : 1	4 : 1	8 : 1
Size (nm)	544.5 ± 16.5	526.8 ± 11.3	488.6 ± 12.9	412.9 ± 15.1	387.4 ± 12.5	334.2 ± 17.4	322.8 ± 21.6
Zeta potential (mV)	+13.6 ± 0.7	+17.6 ± 0.6	+23.1 ± 0.7	+26.8 ± 0.5	+28.1 ± 0.7	+27.4 ± 0.8	+27.6 ± 1.2

was less than 1 : 1. This result indicated that the increase in chitosan concentration could increase the encapsulation efficiency. Consistent with our results, Xu and Du [12] have reported that EE% was highly increased by an increase in the chitosan to BSA concentration, when BSA was used as a model protein. However, there are also contrary reports that show that the increase in chitosan to BSA concentration resulted in EE% decrease [13]. One possible reason is that the increase in chitosan concentration might lead to the increase in the viscosity of chitosan mixture and cause the failure of the combination of protein to chitosan [14]. Furthermore, some studies report that when the chitosan initial concentration is less than 4 mg/ml, EE% increases along with the increase in chitosan to protein concentration, whereas when the chitosan concentration is more than 4 mg/ml, EE% would decrease [15]. Based on previous reports and our own results, we choose 2 mg/ml as the chitosan concentration. In addition, since Alphastatin will be relatively less as the increased ratio of CS/Alphastatin, 1 mg/ml was chosen as Alphastatin concentration (CS/Aphastatin ratio = 2 : 1).

3.2. The Effect of the CS/Alphastatin Ratio on Characteristics. The average particle size and zeta potential of Cs NPs were 305.1 ± 13.8 nm and +26.5 ± 1.1 mV, respectively. When Alphastatin was loaded, the particle size of AsCs NPs increased when the chitosan concentration was 2 mg/ml. Table 1 shows the effect of different mass ratios of chitosan to Alphastatin on particle size at pH 5. The particle size increased with the decrease of the ratio. This indicated that Alphastatin played a part in the ionic cross-linking. In a strict

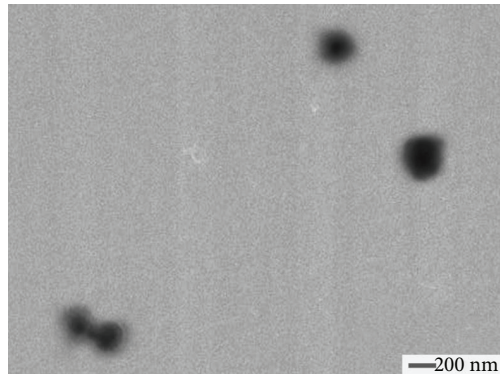

Figure 2: The transmission electron micrographs of AsCs NPs at the mass ratio of chitosan to Alphastatin on 2 : 1.

definition, the particle size of the nanomaterial should be between 1 and 100 nm [16], but the diameter of the nanoparticles made by polymer material may be larger than 100 nm, ranging from 10 to 500 nm, and cannot exceed 1000 nm [17]. In this study, AsCs NPs at the mass ratio of 2 : 1 were still nanoparticles since their average particle size was 387.4 ± 12.5 nm. There is little effect on zeta potential with the increase of the mass ratio from 1 : 1 to 8 : 1, and the AsCs NPs displayed a positive zeta potential in the range of +26 to +28 mV (Table 1). However, at the mass ratio from 1 : 1.5 to 1 : 4, the zeta potential decreased from +23.1 ± 0.7 mV to +13.6 ± 0.7 mV with the decrease of the ratio although they were still the positive zeta potential, which indicated that the negative charge of Alphastatin interacted with the

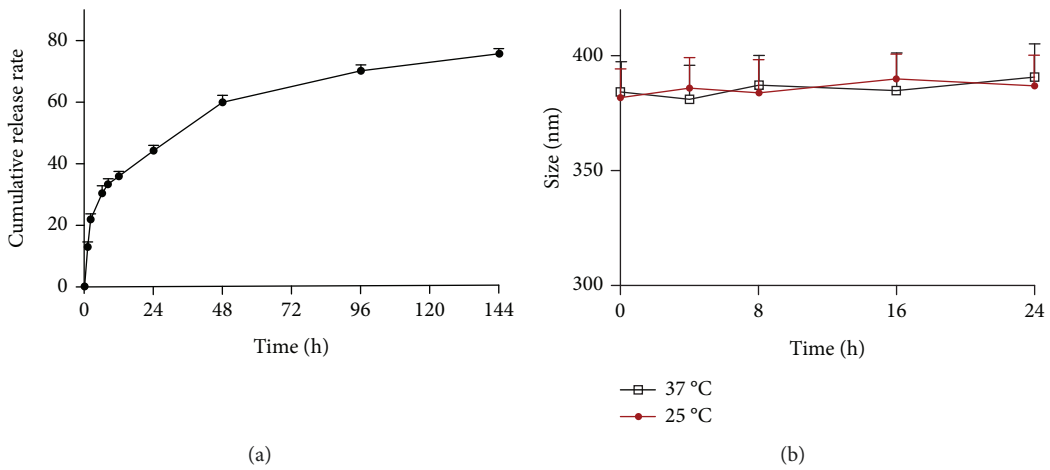

Figure 3: *In vitro* drug release characteristics of AsCs NPs. (a) Cumulative release of AsCs NPs in PBS (pH = 7.4). (b) 24-hour stability study of AsCs NPs in 10% FBS.

positive charge of chitosan via ionic cross-linking. In addition, at the specified mass ratio of 2 : 1, the zeta potential of AsCs NPs was +28.1 ± 0.7 mV (Table 1), and the polydispersity index was 0.223 ± 0.06. And Figure 2 presents the TEM morphology of the AsCs NPs and confirmed the spherical shape. These particles had a small size range of around 270–420 nm in diameter, which was consistent with the result from the particle size analyzer.

3.3. Release and Protection to Alphastatin by AsCs NPs In Vitro. As shown in Figure 3(a), the cumulative release (%) of Alphastatin was from 13.1% to 76.2%. At the first 6 hours, 30.5% Alphastatin was released, and at 12 hours, the cumulative release reached 35.9%, whereas 44.3% Alphastatin was released at 24 hours. This indicated a rapid initial burst release in AsCs NPs. The release decreased to a slower rate at some later stages since 24 hours, with a cumulative release of 60.1% at 48 hours and 70.5% at 96 hours. Then, AsCs NPs were released continuously for 6 days. Because FBS contains a variety of proteases, AsCs NPs were incubated in DMEM containing 10% FBS at 25 and 37°C, respectively. After 24 hours of incubation, it was observed that there was no obvious flocculus or any precipitates in any mixture. The average particle size of nanoparticles in each mixture decreased little at any intervals within 24 hours, which proved that AsCs NPs could be stably present in a liquid system with various proteases (Figure 3(b)). The integrity of encapsulated Alphastatin and released Alphastatin at 24 hours of release was analyzed by Tris-Tricine-SDS-PAGE (Figure 4). The electrophoresis revealed only a single band in the range of 1.0-3.0 kDa for every sample. The band positions were consistent of all samples indicating the integrity of encapsulated Alphastatin and released Alphastatin. The existence form of the drug in chitosan nanoparticles has been discussed in the previous study [18], including simple adsorption on the surface of nanoparticles, and wrapped in the interior of the nanoparticles. Since a small amount of Alphastatin was simply adsorbed on the surface of the nanoparticles, this led to the occurrence of the burst release in the first 12 hours in

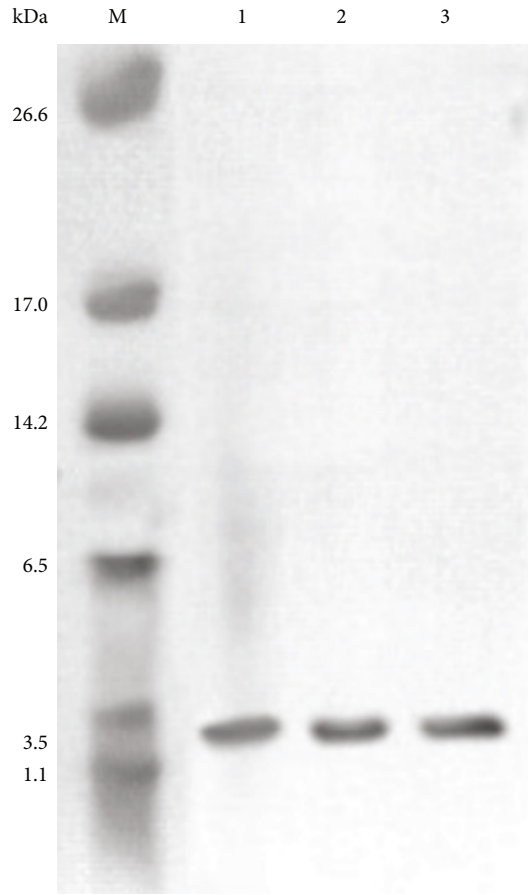

Figure 4: Analysis of Alphastatin integrity by Tricine-SDS-PAGE. M: molecular mass (1060–26,600 Da); 1: AsCs NPs precipitate after a 24-hour release in PBS (pH = 7.4); 2: the supernatant after a 24-hour release of AsCs NPs; 3: the synthetic Alphastatin.

Figure 3(a). Subsequently, Alphastatin inside AsCs NPs was stably released by diffusion through the pores of nanoparticles, and on day 6, 76.2% Alphastatin was released. In a further study, it was observed that after 24 hours of release, both the Alphastatin encapsulated in AsCs NPs and the

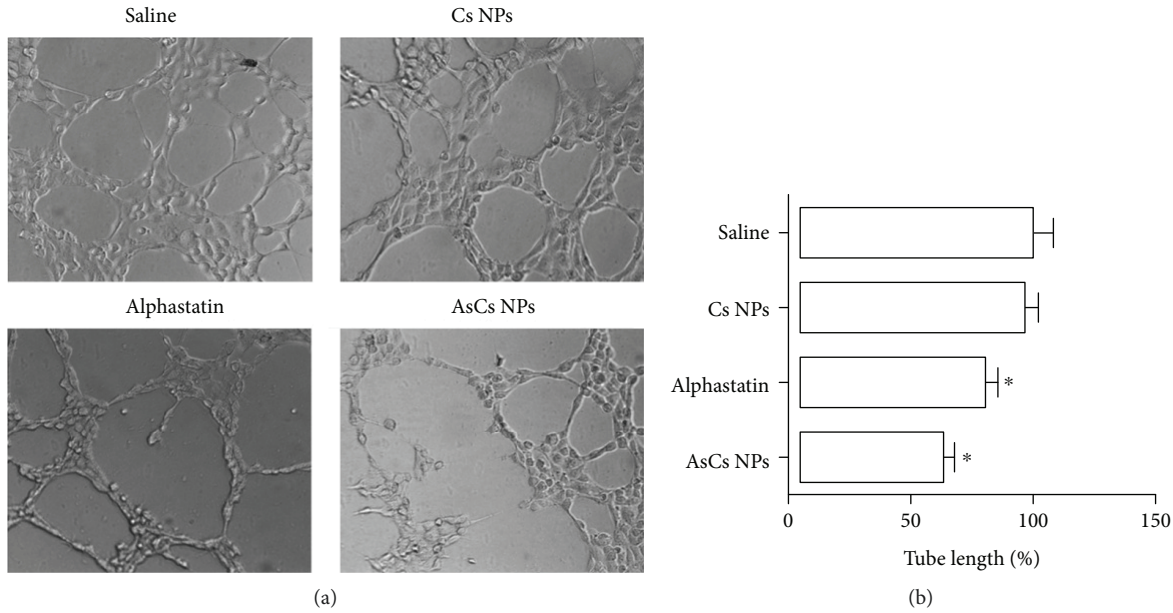

Figure 5: Impact of AsCs NPs on tube formation. (a) Representative images showing HUVEC tube formation under different nanoparticles at 100x magnification. (b) Tube length index. $^{*}P < 0.05$ versus saline control.

released Alphastatin preserved the same molecular mass, indicating the integrity of Alphastatin. For *in vivo* study, the complexity of the circulation system and humoral immune system can affect the stability of nanoparticles. In order to observe whether chitosan could play a basic role in the protection of Alphastatin, FBS was used as a substitute to simulate various proteases [19]. We found that AsCs NPs were stable in the system containing 10% FBS at least 24 hours, suggesting that AsCs NPs may be suitable for *in vivo* administration. Overall, the sustained release and Alphastatin integrity, as well as the stability in serum of AsCs NPs, made the *in vivo* administration possible.

3.4. Inhibition to the Tumor Growth and Angiogenesis In Vivo and In Vitro. It has been reported that Alphastatin inhibits tumor growth mainly by inhibiting the formation of neovasculars in tumors. In order to verify whether AsCs NPs still retained the ability to inhibit tumor growth and angiogenesis, HUVECs and LA975 tumor-bearing mice were used to observe the antiangiogenic effect of AsCs NPs *in vivo* and *in vitro*. As shown in Figure 5(a), in the HUVEC tube formation assay, tubular structures reduced significantly by Alphastatin and AsCs NPs, compared with the saline group. Quantitative analysis (Figure 5(b)) indicated that the tube length was significantly reduced by Alphastatin and AsCs NPs. For the *in vivo* effect of AsCs NPs, we observed that tumor developed in all mice and there was no death in each group. In the saline-treated group (control group), mice moved gradually slowly with tumor growth and presented lack of energy, loss of appetite, and hair loss, whereas mice treated with Alphastatin and AsCs NPs exhibited a better status and did not show the manifestations above. After 14 days of treatment, the tumor weight in all intervention groups was lower than that in the saline-treated group (Figure 6), and the inhibition to tumor growth by AsCs NPs was the strongest

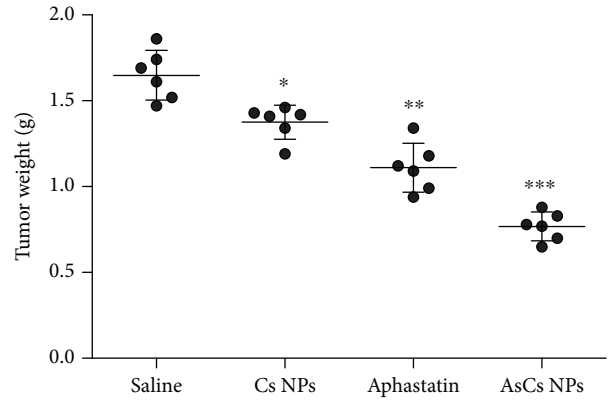

Figure 6: Effects of AsCs NPs on tumor weights from LA975 tumor-bearing mice. $^{*}P < 0.05$, $^{**}P < 0.01$, and $^{***}P < 0.001$ versus saline group.

($P < 0.001$). MVD inside the tumor was further detected. As shown in Figure 7(a), compared with the saline-treated group, the MVD of the AsCs NP ($P < 0.001$) or Alphastatin ($P < 0.05$) group was much lower, and the MVD of the AsCs NP group decreased most obviously. In addition, Figure 7(b) shows that HUVEC tube formation was inhibited by serums containing AsCs NPs ($P < 0.001$) or Alphastatin ($P < 0.05$) after a 2-hour injection, and the serum containing AsCs NPs presented stronger inhibition than did serum containing Alphastatin ($P < 0.001$). In contrast, the serum containing chitosan showed no significant difference in comparison with the blank serum control. It indicated that the increased inhibition by serum containing AsCs NPs could be attributed to the protection of chitosan to Alphastatin. This result is similar to the previous studies [2, 20, 21], indicating that Alphastatin from AsCs NPs could exert the inhibitive ability to angiogenesis both *in vivo* and *in vitro*. Chitosan could inhibit

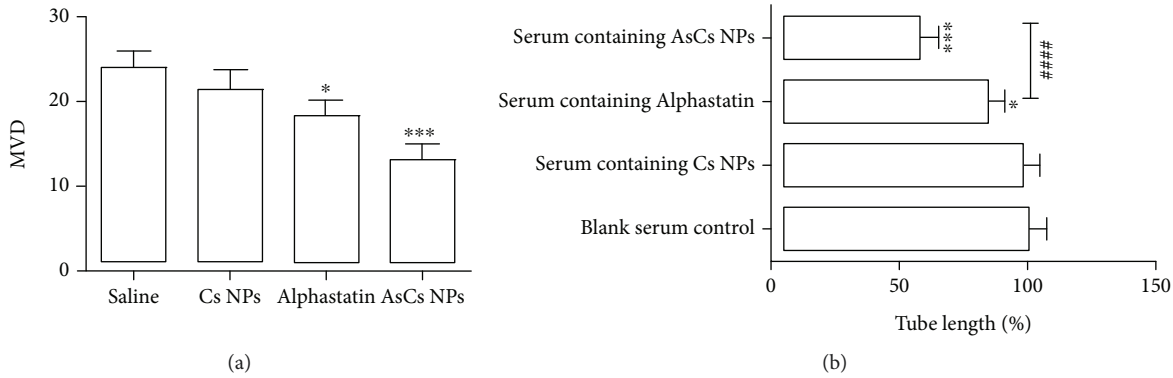

Figure 7: The inhibitory effect on angiogenesis by different nanoparticles. (a) Microvessel density expression in tumor from LA975 tumor-bearing mice treated with different nanoparticles. $^{*}P < 0.05$ and $^{***}P < 0.001$ versus saline group. (b) The inhibitory effect of mouse serums containing drugs against HUVEC tube formation. $^{*}P < 0.05$ and $^{***}P < 0.001$ versus blank serum control, $^{\#\#\#}P < 0.001$ versus serums containing Alphastatin.

tumor growth by directly killing and inducing apoptosis of tumor cells or by an indirect effect through improvement of the immune system of the animal model [22, 23]. Therefore, chitosan inhibited tumor weight ($P < 0.05$) in Figure 6, whereas the inhibition to angiogenesis in tumor and HUVECs by chitosan was not statistically different in Figures 5 and 7. It could be explained that the inhibition to tumor growth by chitosan might be by way of other mechanisms except angiogenesis inhibition. Alphastatin has the ability to inhibit tumor angiogenesis and tumor growth. As shown in Figures 5–7, both tumor weights and MVD levels in Alphastatin and AsCs NP groups were significantly lower than those in the saline group. Since Alphastatin has common disadvantages of peptide and protein drugs, such as degradation by proteolytic enzymes, a short half-life, and disability retaining effective concentration in the tumor for a relative long time, it is necessary to develop a protective system from these disadvantages. Compared with the Alphastatin group, both tumor weight and MVD level in the AsCs NP group were much lower, indicating that chitosan could protect Alphastatin from biodegradation and prolong its effect *in vivo*, which might be contributed by the restrained release and relative stability of AsCs NPs in the circulating system. In addition, chitosan nanoparticles allow the permeation and accumulation in certain tumors through the hyperpermeable vasculature existing in solid tumors, and cannot be easily cleared away due to the absence of the tumor's lymphatic drainage, so that Alphastatin might be remained at the tumor site with possible high concentration. This also contributed to the strongest inhibition to tumor weight and MVD by AsCs NPs.

3.5. SphK1 Inhibition by AsCs NPs. As shown in Figure 8, compared to the saline group, western blot analysis showed that chitosan did not affect the expression level of SphK1, whereas AsCs NPs and Alphastatin downregulated the expression levels of SphK1 in HUVECs. Notably, AsCs NPs presented more potent inhibition than Alphastatin, indicating that the protective and sustained release of chitosan on Alphastatin and the nanoparticles prolonged the function of Alphastatin. Alphastatin inhibits angiogenesis by inhibiting JNK and ERK kinase activation pathways [24] and the S1P-Akt pathway [20, 21, 25], whereas there was no detectable effect on vessels in normal tissues such as the liver, lungs, and kidney [2, 26]. SphK1 phosphorylates sphingosine (Sp) to produce S1P, a key enzyme responsible for the formation of sphingosine-1-phosphate (S1P) [27]. S1P binds to G protein-coupled receptors (GPCRs) on endothelial cell membranes, especially endothelial differentiation gene 1 (EDG-1) which is a member of the S1P receptor family and is essential for vascular maturation. S1P-binded EDG-1 stimulates the synthesis of DNA in vascular endothelial cells and induces vascular endothelial cell migration [28]. The migration of vascular endothelial cells stimulated by SIP was even stronger than that stimulated by basic fibroblast growth factor (bFGF) and vascular endothelial growth factor (VEGF). Moreover, S1P can significantly promote the formation of tubular structures made by endothelial cells and participate in many other important processes of angiogenesis [29]. Thus, the decrease in S1P production will reduce the migration of vascular endothelial cells and the formation of tubular structures. SphK1 is the most important enzyme for S1P synthesis and present positive stimulation to S1P production. AsCs NPs exhibited an inhibitory effect on SphK1, which in turn might inhibit the S1P level. It might be a possible mechanism of inhibitive angiogenesis by AsCs NPs.

3.6. Preliminary Safety Evaluation of AsCs NPs. The blood compatibility of AsCs NPs was evaluated by the hemolysis analysis (Figure 9). The hemolytic effects of both Cs NPs and AsCs NPs were lower than 5% within the range of 0.025–0.1 mg/ml. Because the <5% hemolysis percentage is considered as a safe level [30], the hemolysis results demonstrated that Cs NPs and AsCs NPs had good hemocompatibility and were suitable for intravenous administration.

4. Conclusion

In this study, a chitosan nanoparticle loaded with Alphastatin was prepared with optimization of the mass ratio of chitosan to Alphastatin. Then, the nanoparticle's characteristics were determined. Because of the characteristics

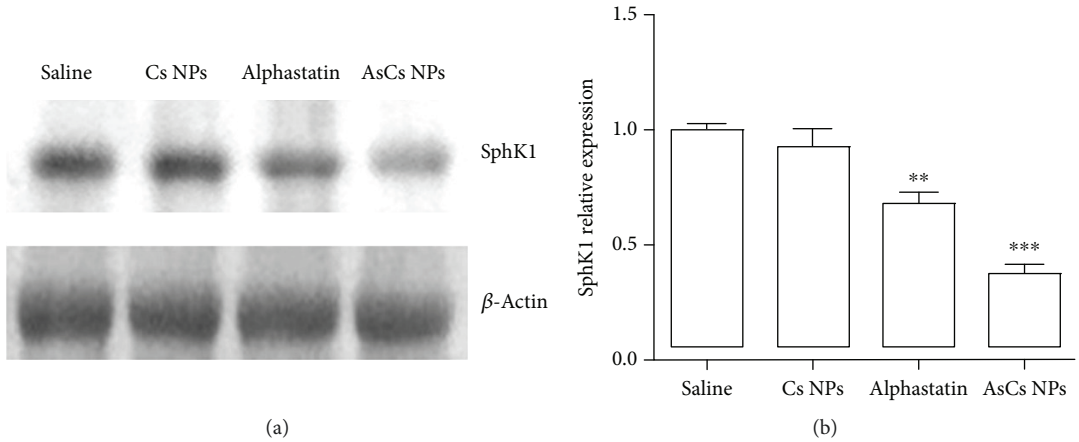

Figure 8: The downregulated SphK1 expression by AsCs NPs was detected by western blotting assay. (a) Representative images of SphK1. (b) The bar graphs show quantified levels of SphK1. $^{**}P < 0.01$ and $^{***}P < 0.001$ versus saline control.

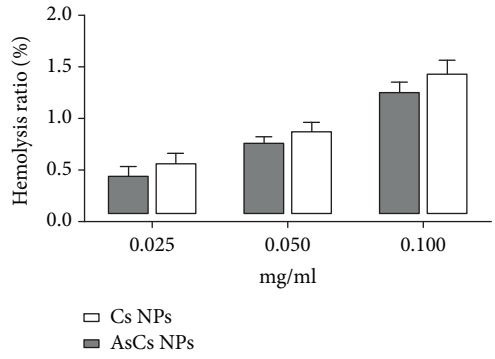

Figure 9: *In vitro* hemolysis assay of AsCs NPs. Hemolysis ratio of polymers at different concentrations.

including the restrained release, the stability in 10% FBS, and the remaining activity in serum-containing drugs, these nanoparticles present considerable antiangiogenic effects *in vivo* and *in vitro*. Additionally, the nanoparticles also present good hemocompatibility. Overall, chitosan could be used as a delivery carrier to strengthen the antitumor effect of Alphastatin.

Data Availability

All raw data used and analyzed during the current study can be available from the corresponding author on reasonable request.

Conflicts of Interest

The authors have no conflicts of interest regarding the publication of this paper.

References

[1] S. Sun and J. H. Schiller, "Angiogenesis inhibitors in the treatment of lung cancer," *Critical Reviews in Oncology/Hematology*, vol. 62, no. 2, pp. 93–104, 2007.

[2] C. A. Staton, N. J. Brown, G. R. Rodgers et al., "Alphastatin, a 24–amino acid fragment of human fibrinogen, is a potent new inhibitor of activated endothelial cells in vitro and in vivo," *Blood*, vol. 103, no. 2, pp. 601–606, 2004.

[3] C. A. Bootle-Wilbraham, S. Tazzyman, J. M. Marshall, and C. E. Lewis, "Fibrinogen E-fragment inhibits the mi-gration and tubule formation of human dermal microvascular endothelial cells in vitro," *Cancer Research*, vol. 60, no. 17, pp. 4719–4724, 2000.

[4] H. Che, J. Song, S. Guo, W. Wang, and G. Gao, "Inhibition of xenograft human glioma tumor growth by lentivirus-mediated gene transfer of alphastatin," *Oncology Reports*, vol. 29, no. 3, pp. 1101–1107, 2013.

[5] S. W. Guo, H. M. Che, and W. Z. Li, "Construction of recombinant lentivirus vector for tumor vasoinhibitory peptide alphastatin gene delivery," *Molecular Medicine Reports*, vol. 3, no. 6, pp. 923–928, 2010.

[6] K. C. Carter and M. Puig-Sellart, "Nanocarriers made from non-ionic surfactants or natural polymers for pulmonary drug delivery," *Current Pharmaceutical Design*, vol. 22, no. 22, pp. 3324–3331, 2016.

[7] M. Amidi, E. Mastrobattista, W. Jiskoot, and W. E. Hennink, "Chitosan-based delivery systems for protein therapeutics and antigens," *Advanced Drug Delivery Reviews*, vol. 62, no. 1, pp. 59–82, 2010.

[8] H. Schägger and G. von Jagow, "Tricine-sodium dodecyl sulfate-polyacrylamide gel electrophoresis for the separation of proteins in the range from 1 to 100 kDa," *Analytical Biochemistry*, vol. 166, no. 2, pp. 368–379, 1987.

[9] E. Jusufović, M. Rijavec, D. Keser et al., "let-7b and miR-126 are down-regulated in tumor tissue and correlate with microvessel density and survival outcomes in non–small–cell lung cancer," *PLoS One*, vol. 7, no. 9, article e45577, 2012.

[10] M. A. Mohammed, J. T. M. Syeda, K. M. Wasan, and E. K. Wasan, "An overview of chitosan nanoparticles and its application in non-parenteral drug delivery," *Pharmaceutics*, vol. 9, no. 4, 2017.

[11] N. Shen, R. Zhang, H. R. Zhang et al., "Inhibition of retinal angiogenesis by gold nanoparticles via inducing autophagy," *International Journal of Ophthalmology*, vol. 11, no. 8, pp. 1269–1276, 2018.

[12] Y. Xu and Y. Du, "Effect of molecular structure of chitosan on protein delivery properties of chitosan nanoparticles," *International Journal of Pharmaceutics*, vol. 250, no. 1, pp. 215–226, 2003.

[13] W. Yang, J. Fu, T. Wang, and N. He, "Chitosan/sodium tripolyphosphate nanoparticles: preparation, characterization and application as drug carrier," *Journal of Biomedical Nanotechnology*, vol. 5, no. 5, pp. 591–595, 2009.

[14] Q. Gan and T. Wang, "Chitosan nanoparticle as protein delivery carrier—systematic examination of fabrication conditions for efficient loading and release," *Colloids and Surfaces B: Biointerfaces*, vol. 59, no. 1, pp. 24–34, 2007.

[15] Z. Liu, Y. Jiao, F. Liu, and Z. Zhang, "Heparin/chitosan nanoparticle carriers prepared by polyelectrolyte complexation," *Journal of Biomedical Materials Research Part A*, vol. 83A, no. 3, pp. 806–812, 2007.

[16] The European Commission, "Commission recommendation of 18 October 2011 on the definition of nanomaterial (2011/696/EU)," *Official Journal of the European Union*, vol. L, no. 275, pp. 38–40, 2011.

[17] R. L. Heise, B. Adam Blakeney, and R. A. Pouliot, "Polymers in tissue engineering," in *Advanced Polymers in Medicine*, F. Puoci, Ed., Springer, Cham, Switzerland, 2015.

[18] S. A. Agnihotri, N. N. Mallikarjuna, and T. M. Aminabhavi, "Recent advances on chitosan-based micro- and nanoparticles in drug delivery," *Journal of Controlled Release*, vol. 100, no. 1, pp. 5–28, 2004.

[19] B. Shahbazi, M. Taghipour, H. Rahmani, K. Sadrjavadi, and A. Fattahi, "Preparation and characterization of silk fibroin/oligochitosan nanoparticles for siRNA delivery," *Colloids and Surfaces B: Biointerfaces*, vol. 136, pp. 867–877, 2015.

[20] T. Li and L. Chen, "Alphastatin inhibits tumor angiogenesis in nude mice bearing human gastric cancer xenografts," *Zhonghua Wei Chang Wai Ke Za Zhi*, vol. 12, no. 1, pp. 61–64, 2009.

[21] L. Chen, T. Li, R. Li, B. Wei, and Z. Peng, "Alphastatin downregulates vascular endothelial cells sphingosine kinase activity and suppresses tumor growth in nude mice bearing human gastric cancer xenografts," *World Journal of Gastroenterology*, vol. 12, no. 26, pp. 4130–4136, 2006.

[22] B. B. Aam, E. B. Heggset, A. L. Norberg, M. Sørlie, K. M. Vårum, and V. G. H. Eijsink, "Production of chitooligosaccharides and their potential applications in medicine," *Marine Drugs*, vol. 8, no. 5, pp. 1482–1517, 2010.

[23] H. T. Ta, C. R. Dass, and D. E. Dunstan, "Injectable chitosan hydrogels for localised cancer therapy," *Journal of Controlled Release*, vol. 126, no. 3, pp. 205–216, 2008.

[24] S. W. Guo, H. M. Che, and W. Z. Li, "Anti-tumor effect of lentivirus-mediated gene transfer of alphastatin on human glioma," *Cancer Science*, vol. 102, no. 5, pp. 1038–1044, 2011.

[25] L. Chen, T. Li, R. Li et al., "Inhibition of alphastatin on angiogenesis in human endothelial cells and the mechanism thereof: an experimental study," *Zhonghua Yi Xue Za Zhi*, vol. 86, no. 15, pp. 1061–1064, 2006.

[26] C. A. Staton, S. M. Stribbling, C. García-Echeverría et al., "Identification of key residues involved in mediating the in vivo anti-tumor/anti-endothelial activity of Alphastatin," *Journal of Thrombosis and Haemostasis*, vol. 5, no. 4, pp. 846–854, 2007.

[27] D. Hatoum, N. Haddadi, Y. Lin, N. T. Nassif, and E. M. McGowan, "Mammalian sphingosine kinase (SphK) isoenzymes and isoform expression: challenges for SphK as an oncotarget," *Oncotarget*, vol. 8, no. 22, pp. 36898–36929, 2017.

[28] Y. Takuwa, H. Okamoto, N. Takuwa, K. Gonda, N. Sugimoto, and S. Sakurada, "Subtype-specific, differential activities of the *EDG* family receptors for sphingosine-1-phosphate, a novel lysophospholipid mediator," *Molecular and Cellular Endocrinology*, vol. 177, no. 1-2, pp. 3–11, 2001.

[29] O. H. Lee, Y. M. Kim, Y. M. Lee et al., "Sphingosine 1-phosphate induces angiogenesis: its angiogenic action and signaling mechanism in human umbilical vein endothelial cells," *Biochemical and Biophysical Research Communications*, vol. 264, no. 3, pp. 743–750, 1999.

[30] Y. Xiao, Y. Liu, S. Yang et al., "Sorafenib and gadolinium co-loaded liposomes for drug delivery and MRI-guided HCC treatment," *Colloids and Surfaces B: Biointerfaces*, vol. 141, pp. 83–92, 2016.